Proceedings of the ASME 2010 3rd Joint US-European Fluids Engineering Summer Meeting and 8th International Conference on Nanochannels, Microchannels, and Minichannels
FEDSM-ICNMM2010
August 1-5, 2010, Montreal, Canada

FEDSM-ICNMM2010-30692

EVALUATING CFD MODELING OF A THERMAL STORAGE UNIT

Monica F. Bonadies, Son H. Ho, J.S. Kapat
Center for Advanced Turbines and Energy Research
University of Central Florida
Orlando, FL, 32816 USA

ABSTRACT

When collecting the energy of the sun for domestic use, there are several options, which include photovoltaic cells and evacuated tube collectors. Arrays of evacuated tube collectors are used to heat water for domestic applications, supplementing the use of a typical hot water heater, while photovoltaic cells transform the sun's radiation into electricity. The benefit of the tube collectors is that they supplement an appliance that uses a fairly large amount of electricity when compared to others in an average home. However, the collectors cannot operate during the night time and produce more hot water than needed at their peak operation point. A thermal storage unit can be used to even out the conversion of energy throughout the day to solve this problem. This study proposes a system using paraffin wax to store thermal energy collected during the day by melting the wax. The system makes use of a finned heat exchanger, with paraffin wax on the shell side, and glycol on the tube side as the heat transfer fluid. It also includes a separate loop for water to flow through and receive thermal energy from the melted wax. Although the wax used in the study is quite effective at storing thermal energy, it has the problem of low conductivity. So, fins are added to the storage and extraction loops to increase the wax's thermal conductivity. The fins not only help to melt the wax more quickly but also act as nucleation sites when the wax freezes. Once all the wax is melted, energy can be exchanged from it to heat water. When creating such a unit, it is useful to have simulation tools to guide its design. One such tool is FLUENT, which will be used in this study to create a simulation of part of the unit. The simulation will be compared to experimental data from a prototype unit and evaluated based upon its strengths and weaknesses.

NOMENCLATURE

PCM	=	phase change material
TC	=	thermocouple

INTRODUCTION

Solar energy has been used for many years to make use of the energy that falls to earth each day from the sun. The collection methods vary from photovoltaic cells to evacuated tubes to parabolic dish collectors at the largest scale. The benefit of using solar thermal as opposed to photovoltaic is that a solar thermal plant produces steam, which is then used in a steam turbine – an already existing technology with several decades of improvement [1]. Furthermore, a smaller scale amount of solar thermal collectors can be used for home hot water heating through a heat exchange system. This provides an alternative to the conventional hot water heater, which makes up a significant portion of a typical family's electricity usage [2].

The use of solar energy has the benefit of being environmentally friendly in terms of nearly zero carbon emissions, but has the drawback of only being available while the sun shines. This means that there is a benefit in adding a storage unit for minimal interruption in the thermal energy supply [3]. The most compelling reason to use thermal energy

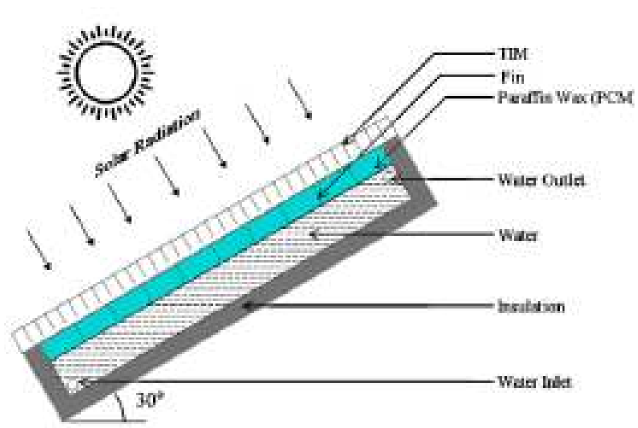

Figure 1: Thermal Storage with Internal Fins [5]

storage is the fact that the storage unit effectively evens out the thermal energy available over a day, since it stores the energy in excess of that which is used during the day. Solar energy is opportunistic – the collection system must be able to take advantage of the energy while it is available. For instance, the maximum solar radiation may occur at mid-day, but the hot water need at that time is not necessarily the greatest. So, the excess radiation can be stored in a solar thermal unit to provide hot water in the evening.

Storage media is divided into two main groups: sensible heat storage and latent heat storage. Sensible heat storage has been implemented in terms of heated tanks of water or beds of rock underneath a home, but latent heat storage provides a unique benefit via its phase change. During a phase change process, the temperature remains constant and the energy received by the medium melts it. With this fact, it is evident that the latent heat storage provides more energy storage than a sensible heat storage unit of the same volume. There are three necessary components in a latent heat energy storage system: a suitable PCM, a suitable heat exchange surface, and a suitable vessel that is compatible with the PCM. The materials available for this application may be organic (such as paraffin wax), inorganic (such as molten salts), or a combination of both (such as a graphite matrix impregnated with paraffin wax). In this study, an organic material, paraffin wax, is used. The structure of paraffin wax is a chain of n-alkanes, and the melt point and latent heat of fusion increase with chain length [4].

Modeling of a phase change material within a storage configuration can be done analytically or numerically, with advantages and disadvantages corresponding to each. These will be explained in specific detail along with an example of application of these methods, but the main advantage of using an analytical or numerical model is that a design can be quickly analyzed, compared to the time it takes to construct a prototype. Numerous analytical and numerical models exist, with their main differences being the design of the method of heat exchange from the working fluid of the solar thermal system to the phase change material. Commerical codes such as FLUENT have also been developed to solve the Navier-Stokes equation as well as give a visual representation of the temperature distribution within the phase change material, as well as the melt fraction of the phase change matieral. For this study we will use the numerical methods of FLUENT.

One of the simplest forms of enhancing thermal conductivity is the addition of rectangular fins within the phase change material. Of course, the configuration and number of fins must be optimized so that natural convection, which speeds the melting process, can take place. Also, the fins cannot be too far apart, as this would create too big an area for them to transfer heat across. Reddy [5] studied the configuration of rectangular fins within an integrated collector system with paraffin wax with embedded fins set beneath a specially coated piece of glass, as shown in Figure 1. Solar radiation would be trapped beneath this glass and the thermal energy transferred to the paraffin wax. The wax in turn would transfer heat to the water bath beneath it, which would be pumped in during the night time. The entire unit was tilted to optimize the sun's position in the sky as well. Once the boundary conditions and heat loss values were determined for this configuration, FLUENT was used to numerically analyze the temperature distributions for 0, 4, 9, and 19 fins within the paraffin wax.

FLUENT does not directly give the location of the melting front, however. Instead, a mushy region can be tracked, with 0 being completely solid material and 1 being a completely melted material. This modeling method was used along with a sinusoidal heat transfer to represent the daily variation of the sun. Results can be shown in terms of temperature contours and liquid fraction variations, which can be given after a certain amount of time. The most important result was that the nine-fin configuration maintained the best heat level, allowed for the maximum amount of natural convection, and had the highest average water temperature and lowest night time temperature drop. This study shows that although placing fins in the phase change material does increase its thermal conductivity, there is a maximum amount of fins one can use to optimize the performance of the storage unit.

FLUENT has also been analyzed in terms of its method of solving phase change problems. Pinelli et al [6] identified the fact that FLUENT's phase change solving method was meant for a few specific applications, so it must be modified accordingly to solve problems outside that realm of applications. They applied FLUENT in solving a phase change occurring within a cylinder with the top of the cylinder heated at a temperature greater than the melting point of the phase change material. This work's goal is to determine the usefulness of FLUENT when analyzing phase change materials, in this case n-octodecane. The numerical results are compared with existing experimental data first before using the program to analyze a phase change condition. Thus, some tweaking is necessary to utilize the code for this application to a cylinder of

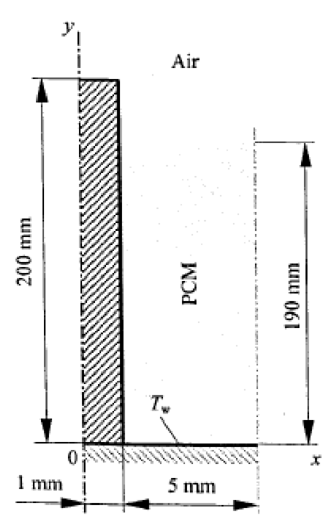

Figure 2: Computational Domain

n-octodecane wax heated from the top with a source of temperature greater than its melting point. The temperature distributions found numerically agreed quite closely with the experimental results previously found by Pinelli. However, the phase change boundary seemed to move more quickly in the numerical model. This difference can be accounted for by the fact that some properties had to be treated as temperature dependent, due to FLUENT's method of handling the phase change – the enthalpy-porosity model was used, with 0 being a solid material and 1 being a fully liquid material. The authors emphasize that the methodology that FLUENT uses should be carefully worked through before using the code, so that the user is aware of the processes. This then allows for changes and assumptions to be made that will help to arrive at a reasonable answer once the code is run.

A partitioned storage unit using aluminum for the partitions and Rubitherm 25 for the PCM was studied by Shatikian et. al [7]. This particular storage unit is identified as suitable for a few different applications, such as storing solar thermal energy or dissipating heat from electronics. The unit tested was composed of the paritions and PCM with an air gap left at the top of each partition of PCM to allow for expansion as the PCM melted. A heating or cooling device was placed underneath the base of the unit to conduct either a melting test or a solidification test. FLUENT was used to numerically simulate the melting and solidification process with the unit two dimensionally. The two dimensional slice was taken from the top to bottom of one half of each storage partition. This computational domain is shown in Figure 2. Within FLUENT, the solidification / melting model was used along with the "volume-of-fluid" model. Obviously the solidification / melting model accounts for the phase change of the wax whilst the "volume-of-fluid" model accounts for the fact that there are multiple fluids to be solved during the computational time. FLUENT uses a modified version of the energy equation, in which the enthalpy of the solid and liquid portions of the melting wax are considered, to solve for the solidification or melting process. The model was solved using the time-dependent calculations in FLUENT, and the results compared to the experimental data. It was found that melting of the wax or solidification of the wax begins at the base of the storage unit, which is heated or cooled for each test. This is due to the extra conductivity provided by the partitions and base of the storage unit. In both cases, the heat transfer from the partitions to the PCM or the PCM to the partitions decreases over time due to the decreasing temperature difference between the wax and the partition. Also, heat transfer to or from the air decreases over time in both the solidification and melting cases.

A molten salt storage tank was analyzed during cooldown by Schulte-Fischedick et al [8] to determine how long it would take for localized solidification to occur while the power plant was not in operation. Since explicit test data was not available for comparison to the simulations, they were verified using a simple energy balance. The storage tank studied is similar to those of Solar Two, since it is a proven use of the molten salt storage. The layout of the tank studied can be seen in Figure 3. The main items of interest were the velocity distributuion of the salt due to natural convection, the heat loss through the sides and base of the tank, and the effect on the natural convection due to the existence of several rod heaters to prevent total solidification during an emergency. There were three steps undertaken to model the situation: FEM to determine heat loss using Ansys, 2-D CFD using FLUENT, and finally 3-D CFD using FLUENT. In the FEM simulation, a published correlation was used to account for laminar free convection along a cylindrical wall, which was the case on the inside of the tank. Some approximations were made to account for the amount of insulation around the tank, the convection and conduction on the outside of the tank, and the existence of the rod heaters within the unit. It was also noted for future reference in the study that the tank was considered "empty" when the level of molten salt was just above the impeller of the salt pump. The salt could not go below this level so that it could be pumped at all times. The 2-D and 3-D CFD simulations required that some boundary conditions be adjusted to fit with the available options within FLUENT. For example, the heat flux into the soil from the base of the tank was rearranged so that it could be used with the convection boundary condition in FLUENT. The 2-D model focused on an internal slice of the tank to examine the velocity patterns as well as the effects of heat loss to the sides and base of the tank. The 3-D model was done as a quarter slice of the tank to examine the effect of the rod heaters on the molten salt tempeature distribution. Along with the velocity distribution and effect of the rod heaters, the time it took for local solidification was also calculated in the 2D and 3D CFD cases.

In this study, FLUENT is used to predict the performance of a solar thermal storage unit at a certain level within the unit. This performance will then be compared to thermocouples located within the actual storage unit during melting and freezing processes. Both processes will be modeled in FLUENT, using the 2-D double precision option. The resulting models will be compared to the experimental data and the accuracy of FLUENT with regard to this problem will be determined. The methods in the studies described will be used

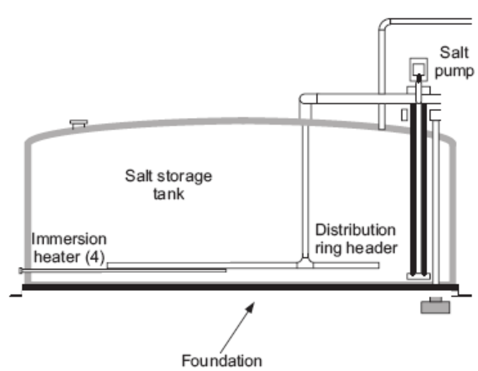

Figure 3: Molten Salt Tank Schematic

as a guide to creating and running the simulations, as well as the help files available from GAMBIT and FLUENT.

METHODOLOGY

Experimental Methods

The experimental setup used to validate the analytical model derived is comprised of an array of twelve thermal energy collection heat pipes from GEAR Solar, two Grundfos pumps to circulate the water and heat transfer fluid, and a collection unit filled with paraffin wax and a copper heat exchanger to store thermal energy. An exterior view of the unit is shown in Figure 4.

Figure 4: Solar Collector and Storage

To determine the effectiveness of the storage unit, it was tested on various days with varying weather conditions to determine the effectiveness of the unit in storing energy, then being able to release it to the heat load. Two main testing methodologies needed to be carried out, the first being the melting of the wax and the second being the freezing of the wax. A city water source was used for the freezing test.

The melting tests were carried out on clear days during the months of November through February. These days were especially good for solar testing due to the low levels of humidity – higher levels of humidity scatter the solar radiation, so a lower level of humidity is desired for testing. Over the range of time chosen for testing, the average ambient temperature was approximately 10°C.

To begin the melting test, the rig was rolled outside and the heat tubes allowed to heat up for half an hour. This allowed the heat tubes to come to approximately 80-90°C before beginning to circulate the heat transfer fluid. This particular heat transfer fluid was ethylene glycol to ensure that it would not boil in the tubes. This boiling was undesirable as it would cause the pump to seize and be damaged. The pump was then turned on and set to a one gallon per minute flow rate. Thermocouples were placed at the inlet and exit of the storage as well as the inlet and exit of the solar collector manifold to read the mean fluid temperature at half hour intervals. They were also embedded within the wax in various locations at two different depths. The depths are shown in Figure 5 and the locations are shown in Figure 6. The depth of 4” above the base of the unit is considered in this study and is denoted by B (for base). The melting test was continued from the morning until the temperature of the fluid exiting the solar thermal heating tube manifold began to drop. Data was taken at half hour intervals during the melting test and fifteen minute intervals during the freezing test.

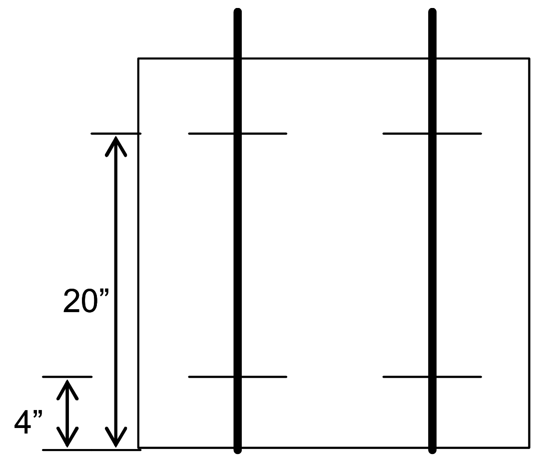

Figure 5: Thermocouple Depths

After some initial data analysis, it was determined that the use of thermocouples at the inlet and exit of the storage was not sufficiently accurate to measure the heat stored by the unit. The thermocouples used were a type T and have only an accuracy of +/- 1° C. Therefore, a thermopile, or a set of thermocouples welded in series, was used at the entrance and exit to the inlet and outlet of the storage unit. There were ten thermocouples on each side, which leads to an uncertainty of 0.1° C. With this method of measurement, the voltage was read from the thermopile and converted to a temperature difference using a calibration curve. This curve was developed using an ice bath for one end of the thermopile and an Omega Precision Temperature Unit. In this way, one end of the thermopile was kept at 0° C while the other was at a known temperature. Data was taken from the thermopile and the thermocouples embedded within the wax and at the exit and entrance of the solar thermal manifold every half hour during the melting test process.

To do the freezing test, a hose with city water access was attached to the heat load loop of the unit (shown in blue in Figure 6), and was turned on. The temperature of the wax and fluid inlet and exit from the heat load loop was noted before the

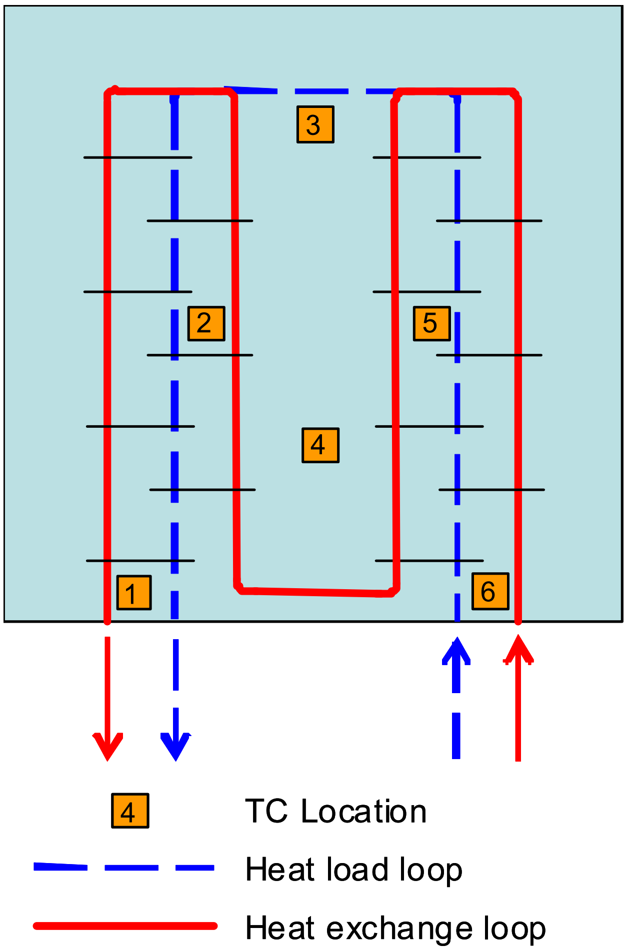

Figure 6: Heat Exchanger Schematic

water was turned on. At the instant the water was turned on and started to come out of the unit within the heat load loop side, the temperature at the exit of the heat load loop was taken. Temperatures were thereafter taken at fifteen minute intervals and continued for an hour. This was found to be the useful limit for extraction of heat; the temperature of the water exiting the rig did not significantly change after that point.

Numerical Methods

The first step in CFD modeling was the creation of a base for the simulation. Drawings created of the test stand were used as a guide to create a two dimensional base for the mesh. There were two loops tested, the heat load and heat transfer loops. While the heat load had water running through it, the heat transfer loop was assumed to have stagnant antifreeze within it, and vice versa while the heat transfer loop was tested. The wax was modeled the same way for both cases.

Next, an appropriate mesh needed to be created for not only the wax but heat transfer fluid as well. Each of these meshes was made with consideration to what could be estimated to occur. For example, the melting front of the wax would be most evident at the outside surface of the pipes and the fins. So, a boundary layer mesh was created at these surfaces. The rest of the wax was meshed after this boundary was created. Furthermore, the mesh was created more tightly around the bends in the piping. A quadrilateral mapped mesh was used wherever possible due to the stabilty of the quad mesh.

There were two different meshes created for the two different cases studied – melting and solidification of the wax. The melting of the wax was started assuming a completely solidified system, while the solidification of the wax was started assuming a completely melted system. For each of these two cases, the fluid not being run in the rig was assumed to be perfectly stagnant, with no fluid entering or exiting the rig. The fluid was meshed, however, to account for any heat transfer to or from it during the process affected more by the other fluid.

To create a two dimensional simulation of the "slice" taken from the heat exchanger, an approximation was made to reflect the fact that the heating and cooling loops can only exchange heat to each other through the fins, due to the design of the heat exchanger. So, an adiabatic wall was placed within the mesh to separate the copper tubing at the point where the heat exchange and head load loops would overlap within the unit.

For the fluid within the tubes of the heat exchanger, the boundary layer mesh was also used where needed to go around the curved portions of the exchanger. This mesh was separated from the wax mesh by the solid copper of the heat exchanger. The copper was indicated as a solid body in GAMBIT and the wax a fluid body before exporting the geometry files to a mesh for transfer to FLUENT.

When running the simulations, several assumptions were made. Firstly, the wax was assumed to be all at the same temperature when the simulation began, whether it was for a melting or freezing simulation. Furthermore, the antifreeze was assumed to be at approximately 75 C at the inlet for all times, as this was the average temperature achieved during the melting process. A similar assumption was made for the incoming water during the discharge process; it was assumed to come in at 20 C for all times. Finally, the section modeled in two dimensions in FLUENT was assumed to correspond with the thermocouples at the 4 inch depth, as their values would be affected somewhat less by gravity than those at the 20 inch depth.

Within FLUENT, several specifications needed to be made as to the solution of the Navier-Stokes and energy equations. The solidification / melting model was enabled, and the default pull value left alone. This value is more for the modeling of casting, which does not apply to this study. The iterations were based largely upon time iteration since the energy equation was solved in approximately two to three iterations as the solution proceeded. The time step was set at one second, and the maximum amount of solution iterations was set at 20. The upwind values and other parameters specific to the solution were kept as first-order or default values to get a baseline case. Once this case has been perfected, these values will be advanced for a more precise solution.

RESULTS

The experimental results are presented first as they are the actual performance of the collection and storage system. The test for validation of the CFD code was conducted at a mass flow rate of 1 gpm through the heat exchange loop (shown in red in Figure 6). This melting test was followed by a freezing test using city water if the wax was at the melting point throughout the storage unit.

The melting process took place over the span of two days using a one gallon per minute flow rate. The dates considered were January 4th and 5th. The melting progress of selected locations within the wax can be seen in Figure 7. The conditions on the two days were sunny and low humidity, as the data was taken during the winter in Florida. The unit takes a total of 13 hours to charge. The charge cutoff point is determined to be when all of the points within the unit reach 50 C, which is the wax melting point quoted by the manufacturer. However, it is also remembered that the melting of the material does not occur ideally due to its impurities. The material used was paraffin wax meant for candles, and therefore did not have a purity guarantee. The impurities in the wax cause it to have a larger range of melting temperatures than a more pure wax.

The experimental melting process and the CFD melting process are within ten degrees of each other for the first seven hours of unit operation, but at the 13 hour mark, the CFD is significantly higher at the 1B and 6B locations. Interestingly, the 4B location is relatively accurate, and it the closest during the entire simulation. This may be due to the fact that location 4 experiences the least bit of temperature change during the entire process, while locations 1 and 6 experience the greatest and least heat transfer due to their location within the storage unit. Location 1 is considered to be at the exit of the heat transfer loop whilst location 6 is at the entrance of the heat transfer loop.

Figure 8 shows the physical process of melting through contours of temperature on the left side of the figure and melt fraction on the right hand side of the figure. The melt fraction ranges from 0 to 1, with 0 being completely frozen material and 1 being completely melted material. The water and ethelyne glycol used do not freeze or melt at any time in the process; they remain at 1 as far as the liquid fraction is concerned. The lower limit of the melting fraction is shown in blue, while the higher limit is shown in red.

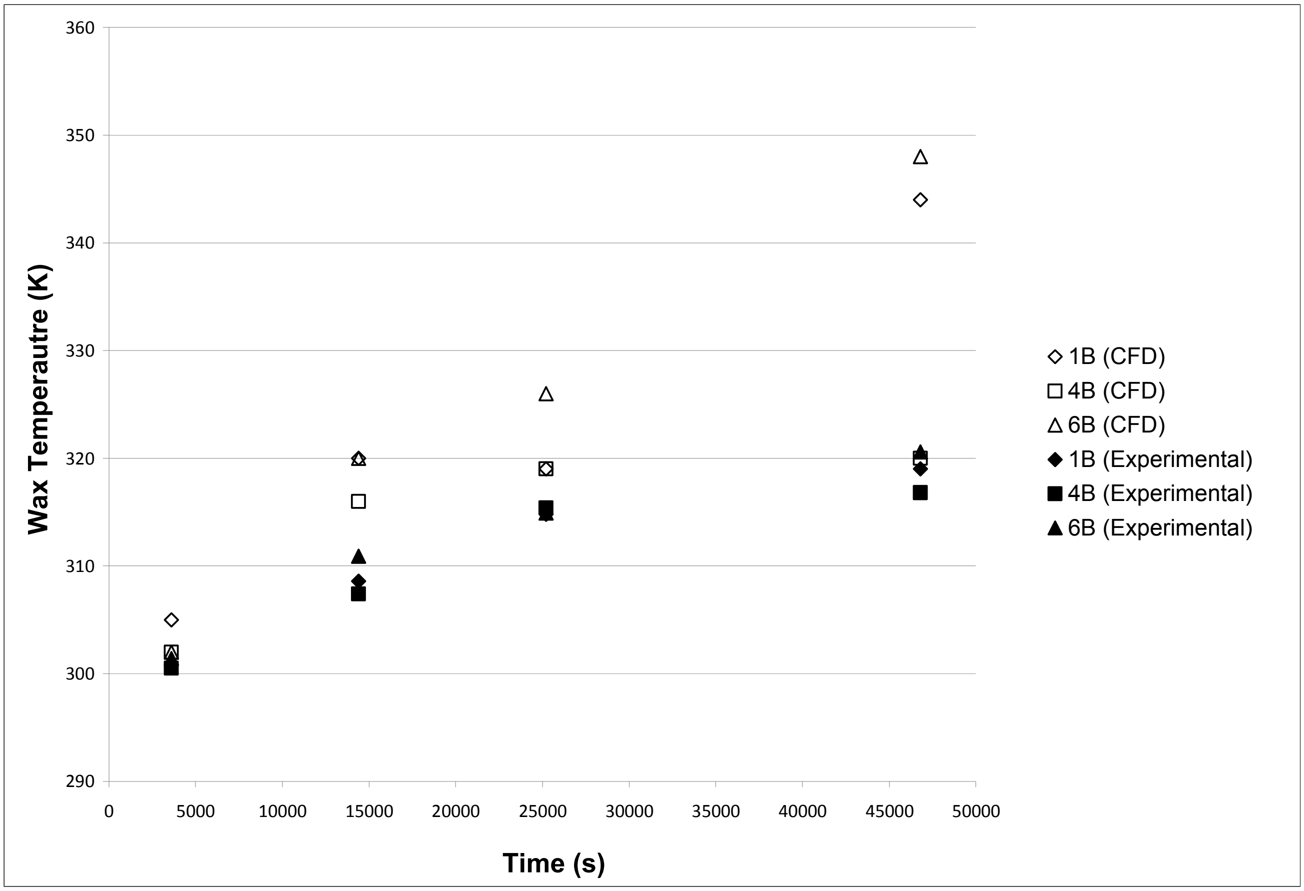

Figure 7: Wax Temperature Distribution During Melting Process

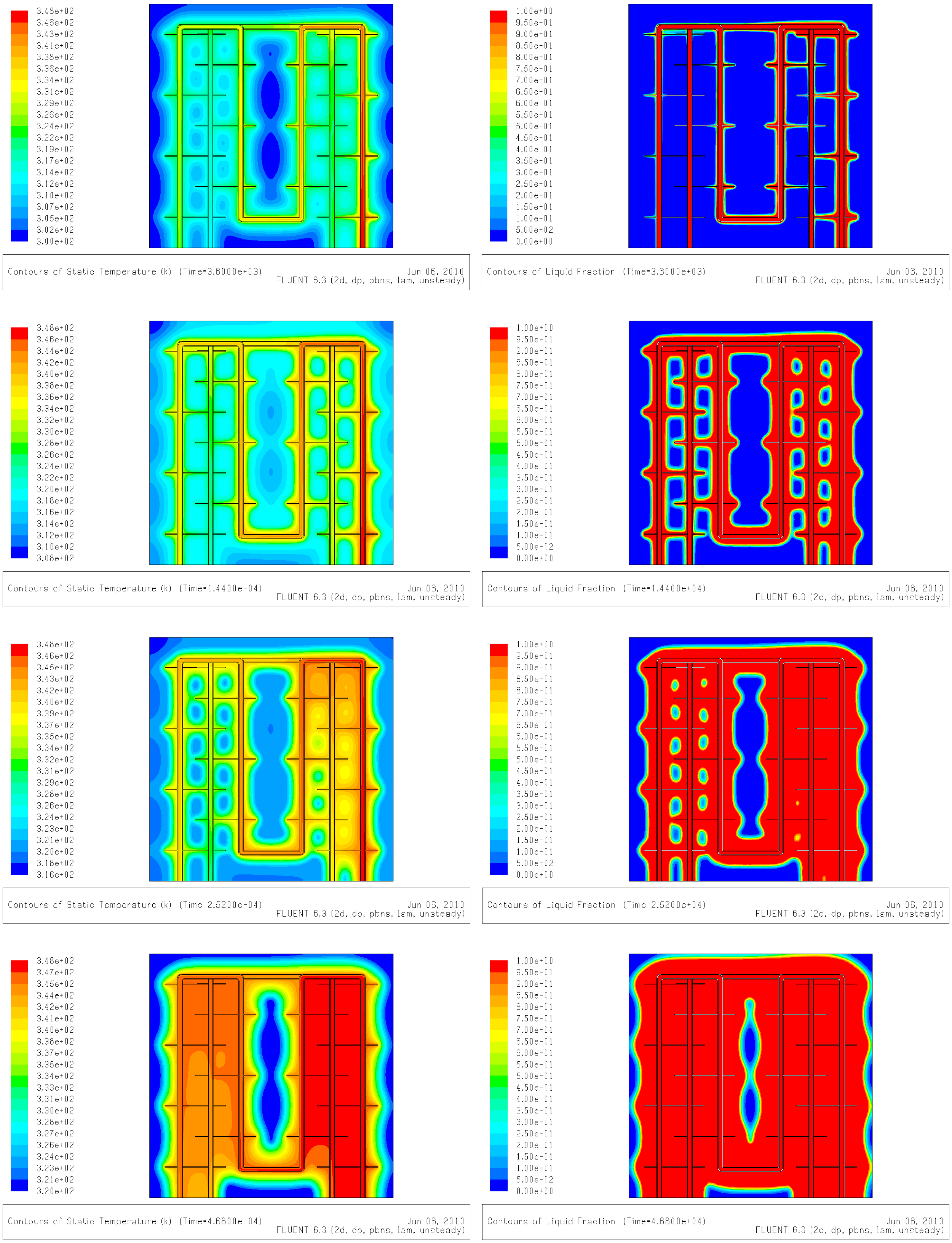

Figure 8: Temperature and Liquid Fraction Progression, Melting Case

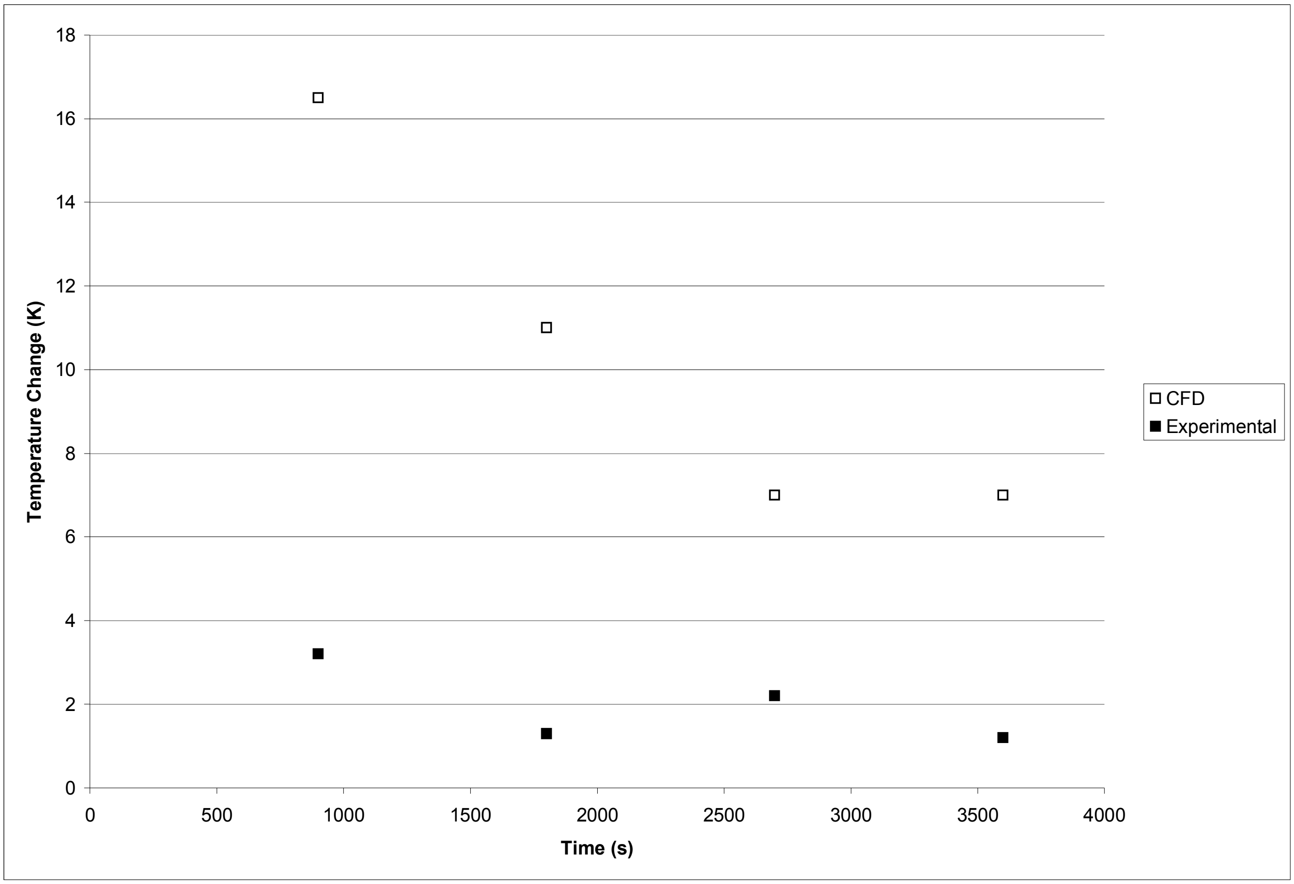

Figure 9: Change in Temperature of Water During Heat Extraction Process

As for the freezing case, the CFD and experimental results do not agree as closely. At most, a temperature change of approximately 3 C was achieved with water at 3 gpm and city pressure. These results can be seen in Figure 9. A slower mass flow rate would be required to extract heat if nothing else on the unit was changed. The water might also have to make more than one pass through the unit to achieve the minimum safe hot water temperature of approximately 50 C (120 F) [9].

The outlet temperature of the water in the CFD model is seven degrees higher than the inlet temperature of the water at 900 seconds, which is approximately twice the increase noted in the experimental data. The fact that the heat transfer to the water in the CFD model is higher than reality makes sense, as the CFD calculates ideal heat transfer. In the experiment, there was heat loss through the aluminum box the wax was encased in, as well as loss to bubbles forming in the city water supply. Considering the wax temperature, the wax was, on average, near the melting point at all data points taken within the storage unit. Comparing this to the same location in the CFD model, the model also has this feature. However, it must also be noted that the wax used within the storage unit was not laboratory grade purity, therefore it has a larger melting point range than the storage unit modeled.

The wax solidification process during the extraction of heat from the wax can be seen in Figure 10. The FLUENT results are presented in a similar way to those of the melting process. It is evident in these simulation results that the fins of the heat exchanger serve as nucleation sites for the freezing process as well as the tubes.

CONCLUSIONS

The results from the two dimensional CFD model of the freezing case are twice as large as the actual results, due to the ideal nature of the model. With this in mind, the model can be used to predict other cases, i.e. other melting temperatures of the wax.

The experimental work with this test rig shows that a full charge is possible during two relatively sunny days, but it would be ideal to have a full charge possible within a day, so that the energy could be put to use more quickly. Furthermore, the freezing process of the wax does not give the necessary hot water temperature for a home. This could be changed either by the increased temperature of the wax melt point or circulation of the water through the exchange loop more than once.

Future work from this paper would include a three dimensional simulation to see the effect of gravity within the rig on the melting and solidification of the wax, since the two dimensional "slices" did not consider gravity. This simulation would focus upon the entrance and exit portions of the test rig, since they most closely inform the melting of the wax and the transfer of heat within the storage unit. Also, a study could be done to determine the ideal number of fins on the heat exchanger.

ACKNOWLEDGMENTS

Monica Bonadies would like to acknowledge financial support in the form of a Provost's Fellowship from the University of Central Florida.

All authors would like to recognize the donation of solar thermal heat collection tubes from Dr. David Lu of GEAR Solar, as well as the donation of pumps from Grundfos. We are also grateful to Dr. Arup Guha of the University of Central Florida for his management of the cluster on which the FLUENT cases were run.

REFERENCES

[1] Johnson, G., "Plugging Into the Sun," National Geographic, September 2009, pp. 28-51.

[2] http://www.energysavers.gov/your_home/water_heating/index.cfm/mytopic=13050, accessed November 16, 2009.

[3] Zalba, B., Marin, J.M., Cabeza, L.F., Mehling, H., 2003, "Review on thermal energy storage with phase change: materials, heat transfer analysis and applications," Applied Thermal Engineering, 23, pp.251-283.

[4] Sharma, A., Tyagi, V.V., Chen, C.R., Buddhi, D., "Review on thermal energy storage with phase change materials and applications," Renewable and Sustainable Energy Reviews, 2009, 13, 318-345.

[5] Reddy, K.S., 2007, "Thermal Modeling of PCM-Based Solar Integrated Collector Storage Water Heating System," J. Solar Energy Engineering, 129, pp. 458-464.

[6] Pinelli, M., Piva, S., 2003, "Solid/Liquid Phase Change in Persence of Natural Convection: A Thermal Energy Storage Case Study," J. Energy Resources

[7] Shatikian, V., Dubovsky, G., Ziskind, G., Letan, R., 2003, "Simulation of PCM Modeling and Solidification in a Partitioned Storage Unit", Proceedings of the ASME Summer Heat Transfer Conference.

[8] Schulte-Fischedick, J., Tamme, R., Hermann, U., 2008, "CFD Analysis of the Cool Down Behaviour of Molten Salt Thermal Storage Systems", Proceedings of Energy Sustainability.

[9] http://www.energy.ca.gov/2005publications/CEC-400-2005-005/chapters_4q/5_Water_Heating_Requirements.pdf, accessed March 23, 2010

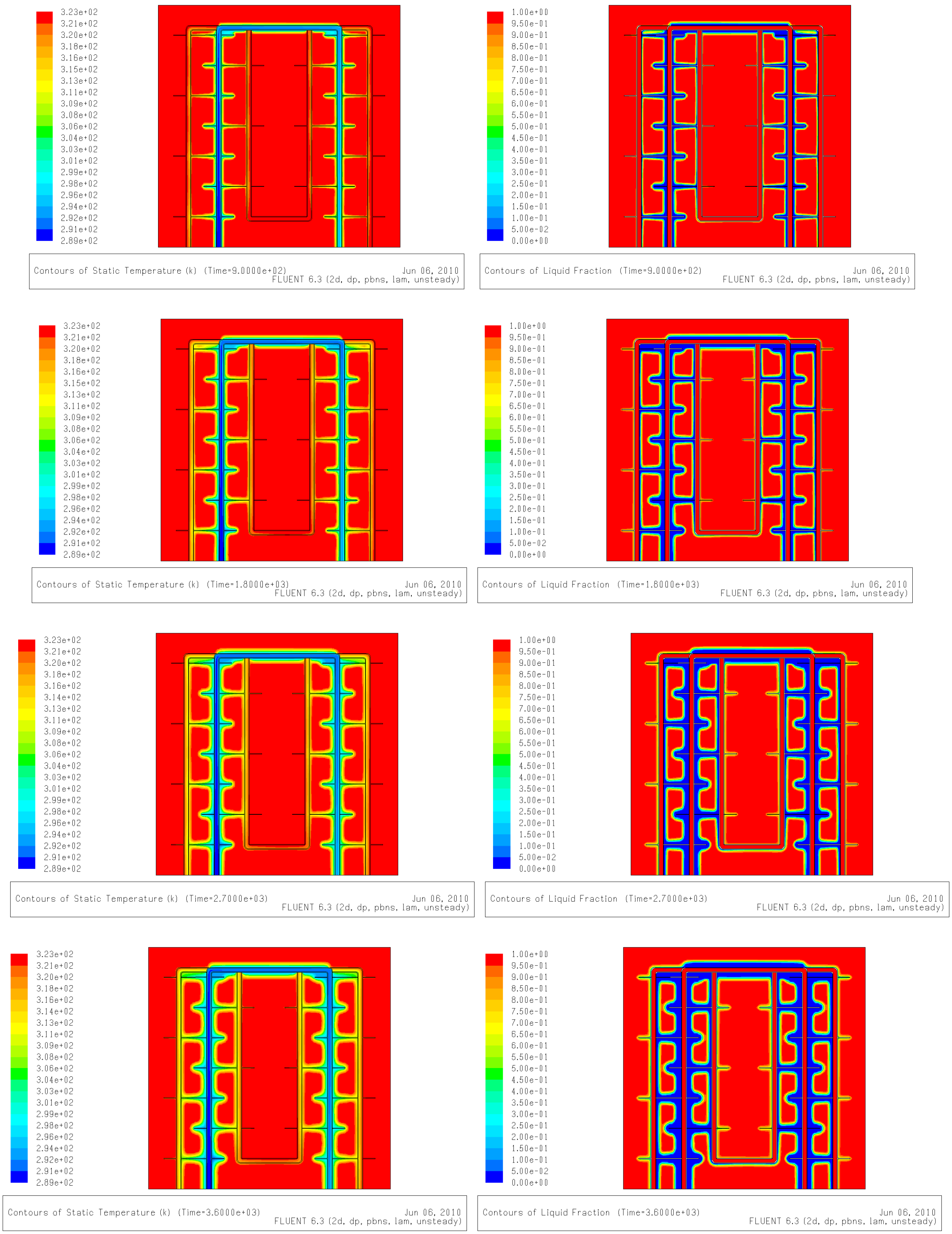

Figure 10: Temperature Distribution and Melt Fraction Progression, Freezing Case